Journal Pre-proof

Biochar-Amended Soils Enhance Drought Resilience in Lettuce: Integrating Hyperspectral Imaging (HSI) and CNN-Based Moisture Prediction

Ruogu Tang, Ashish Reddy Mulaka, Wenxin Rong, Xu Yuan, Yin Bao, Juzhong Tan

PII: S2666-1543(26)00081-5

DOI: https://doi.org/10.1016/j.jafr.2026.102711

Reference: JAFR 102711

To appear in: *Journal of Agriculture and Food Research*

Received Date: 29 October 2025

Revised Date: 18 January 2026

Accepted Date: 22 January 2026

Please cite this article as: R. Tang, A.R. Mulaka, W. Rong, X. Yuan, Y. Bao, J. Tan, Biochar-Amended Soils Enhance Drought Resilience in Lettuce: Integrating Hyperspectral Imaging (HSI) and CNN-Based Moisture Prediction, *Journal of Agriculture and Food Research*, https://doi.org/10.1016/j.jafr.2026.102711.

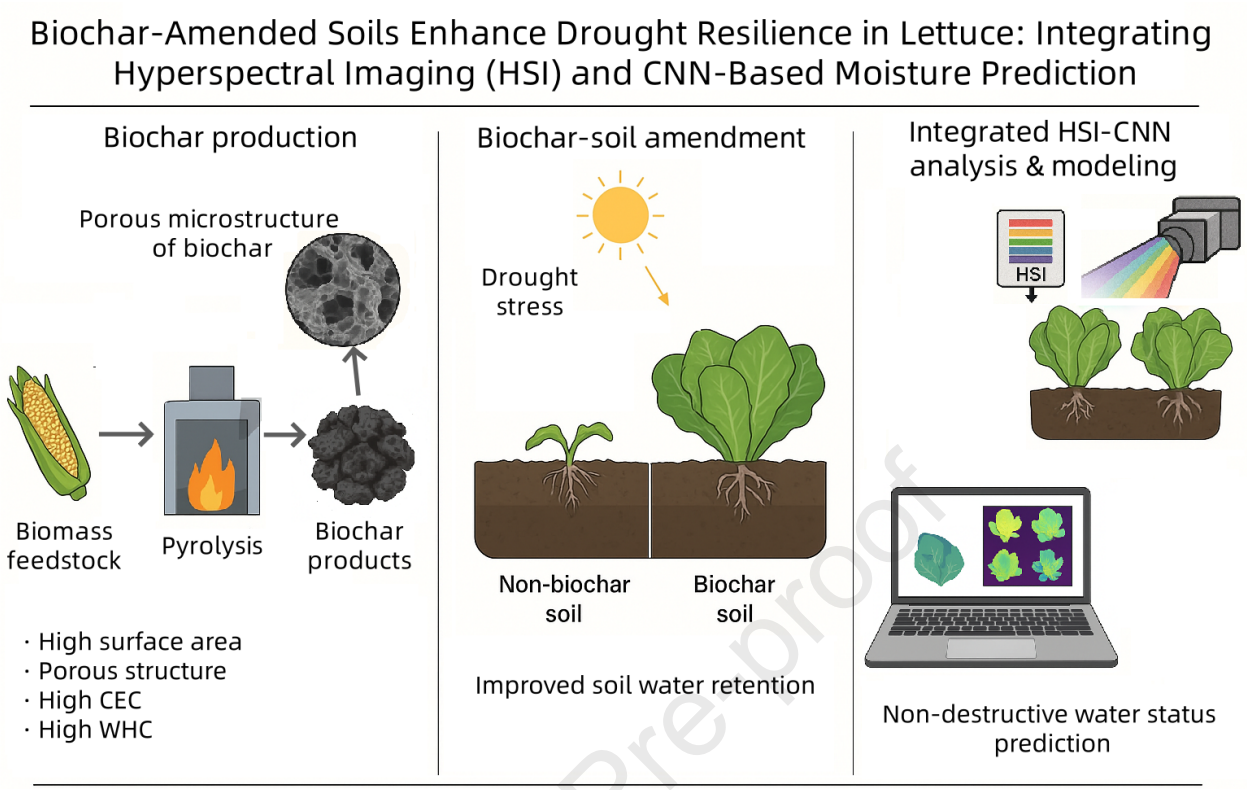

Biochar-Amended Soils Enhance Drought Resilience in Lettuce: Integrating Hyperspectral Imaging (HSI) and CNN-Based Moisture Prediction

Ruogu Tang[1], Ashish Reddy Mulaka[1], Wenxin Rong[2], Xu Yuan[2], Yin Bao[3], and Juzhong Tan [1*]

[1] Department of Animal and Food Sciences, University of Delaware, College of Agriculture and Natural Resources, Newark, DE, USA, 19713

[2] Department of Computer and Information Sciences, University of Delaware, College of Engineering, Newark, DE, USA, 19713

[3] Department of Plant and Soil Sciences, University of Delaware, College of Agriculture and Natural Resources, Newark, DE, USA, 19713

* Corresponding author:
Dr. Juzhong Tan
Department of Animal & Food Sciences
College of Agriculture and Natural Resources
University of Delaware
Newark, DE, 19713
jztan@udel.edu
302-831-6839

Abstract

The increasing frequency and severity of drought events threaten global food security by degrading soil fertility and reducing crop yields. In this study, we employed biochar as a soil amendment to improve soil water-holding capacity and support plant growth under limited irrigation. While biochar offers a practical means to enhance crop performance, its evaluation has traditionally relied on destructive, labor-intensive measurements. Although we confirmed the positive effects of biochar through experimental assessments, we recognized the need for a rapid, non-destructive method to evaluate drought resilience under reduced irrigation more efficiently. To address this demand, we integrated biochar amendments with hyperspectral imaging (HSI) and convolutional neural network (CNN) modeling into a unified agronomic-computational framework. Corn-stalk-derived biochars, produced at 350 ºC, 550 ºC, and 700 ºC and applied at 1%, 3%, 5 wt%, by weight, were tested in lettuce under well-watered and water-stressed conditions. Under drought stress, highly pyrolyzed biochars (CSB550 and CSB700) at 5 wt% increased fresh biomass by 33.2%, plant height by 29.8%, and leaf moisture content by 5.63% relative to the drought-stressed control without biochar amendment, while improving soil moisture retention by up to 24%. Leveraging HSI's rich spectral signatures and CNN's ability to model complex, non-linear relationships, plant moisture content was predicted with an R^2 of 0.93 and RMSE of 0.28%, closely matching destructive measurements. This integrated approach delivers both a practical soil management strategy to mitigate drought impacts and a scalable, high-throughput tool for real-time crop water monitoring, supporting precision irrigation and climate-resilient agriculture.

Keywords: Biochar, drought stress, soil amendment, lettuce growth, machine learning prediction

1. Introduction

Water scarcity is one of the most pressing global challenges, threatening food production, rural livelihoods, and ecosystem stability, particularly in arid and semi-arid regions [1,2,3]. Agriculture accounts for over 70% of global freshwater withdrawals, making it highly vulnerable to the increasing frequency and severity of droughts caused by climate change [3]. This growing imbalance between water demand and availability underscores the urgent need for adaptive and resilient farming practices that can enhance water-use efficiency and sustain crop yields under water-limited conditions [4]. Among horticultural crops, leafy vegetables such as lettuce are especially sensitive to water stress due to their shallow root systems, high transpiration rates, and short production cycles [5]. Even moderate soil moisture deficits can lead to reduced biomass, leaf wilting, and quality deterioration, ultimately affecting both yield and market value [6]. Because of their sensitivity and economic importance, leafy vegetables serve as effective model crops for evaluating soil and management strategies aimed at improving plant water availability and drought resilience.

A variety of agronomic, technological, and policy-driven strategies have been explored to improve drought resilience in agriculture [7,8]. These include optimized irrigation techniques such as drip or deficit irrigation, mulching to reduce surface evaporation [9], the use of synthetic hydrogels or soil conditioners [10], and the breeding or genetic modification of drought-tolerant varieties [11]. Broader initiatives have included subsidies for water-efficient technologies and regulatory measures to promote sustainable water use [12,13]. However, many of these approaches face barriers to widespread adoption, including high installation and maintenance costs, variable performance across soil types and climates, and limited accessibility for smallholder farmers [14]. Additionally, some synthetic soil conditioners pose environmental concerns due to their persistence and low biodegradability [15]. These challenges have driven interest in natural, sustainable soil amendments that enhance water retention and plant performance without compromising environmental integrity.

Among these, biochar has gained attention as a practical amendment for improving soil performance under drought conditions[16]. Produced from biomass via pyrolysis, biochar's high porosity, surface area, and functional group diversity can enhance soil moisture retention, nutrient availability, and microbial activity [16]. These properties depend strongly on feedstock type, pyrolysis temperature, and application rate [17,18], making it essential to understand how these variables affect plant-soil interactions under stress. In controlled environments, biochar application has shown potential to mitigate drought impacts on crop growth, but its benefits are often assessed using traditional approaches that depend on destructive, labor-intensive measurements such as biomass harvesting or oven-dry moisture determination. While these methods yield accurate data, they capture only endpoint results and cannot track plant responses over time, limiting their usefulness for frequent monitoring or large-scale screening. To address this limitation, rapid, non-destructive assessment methods are needed to complement agronomic trials and enable continuous, high-resolution monitoring of plant water status.

Hyperspectral imaging (HSI) is a promising solution, capturing hundreds of contiguous spectral bands that reveal subtle physiological changes associated with water stress-often before visible symptoms appear. When combined with convolutional neural networks (CNNs), which can model complex, non-linear relationships between spectral signatures and plant traits, HSI data can be translated into accurate predictions of leaf moisture content. This capability provides a scalable, treatment-agnostic tool for evaluating drought resilience in real time, bridging the gap between experimental interventions and actionable field monitoring.

The overall objective of this study was to evaluate the potential of biochar amendments to enhance lettuce drought resilience while establishing a non-destructive, data-driven framework for monitoring plant water status under reduced irrigation. To achieve this objective, we tested the hypotheses that (i) biochar properties governed by pyrolysis temperature and application rate influence soil physicochemical characteristics and water-holding capacity, thereby mitigating drought-induced constraints on plant growth and water status, and (ii) hyperspectral imaging combined with convolutional neural network (CNN) modeling can accurately and non-destructively predict leaf moisture content across varying irrigation and biochar treatment conditions. In this study, we integrated biochar amendments with HSI-CNN analytics into a unified agronomic-computational framework. Corn-stalk-derived biochars were produced at three pyrolysis temperatures (350 ºC, 550 ºC, and 700 ºC), characterized for key physicochemical properties, including pH, ash content, elemental composition, surface area, and polycyclic aromatic hydrocarbon (PAH) content. The biochars were then applied to soil at different rates, after which we analyzed the properties of the amended soils, including pH, cation exchange capacity (CEC), water-holding capacity, and mineral nutrient levels. Lettuce was cultivated under well-watered and water-stressed regimes to evaluate the effects of biochar type and application rate on plants. Plant performance was assessed through measurements of fresh and dry biomass, root and shoot length, moisture content, and final yield. Concurrently, HSI data were collected throughout the growth cycle and were used to train and validate a CNN model for non-destructive leaf moisture prediction. By combining a practical soil amendment with a rapid, high-throughput evaluation method, this study not only quantified the drought-mitigating effects of biochar across varying pyrolysis temperatures and application rates, but also demonstrated that HSI-CNN modeling can accurately and non-destructively monitor plant water status in real time. This dual approach established an integrated agronomic-computational framework that links soil management practices directly to plant physiological outcomes, providing both a scalable intervention to enhance drought resilience under reduced irrigation and a decision-support tool for precision irrigation and climate-resilient crop management.

2. Method

2.1 Biochar Materials

Three biochar samples made from corn stalks (CSB350, CSB550, and CSB700), produced at pyrolysis temperatures of 350°C, 550°C, and 700°C, respectively, were used in this study [19]. Detailed procedures for biochar preparation and physicochemical characterization are provided in the Supplementary Information (SI, Section S1).

2.2 Soil amendment by biochar incorporation

Three types of corn biochar-CSB350, CSB550, and CSB700-were ground and sieved to a particle size of <1 mm prior to application. Air-dried loamy soil was used as the growth substrate and passed through a 2 mm mesh to ensure uniformity. Each biochar type was incorporated individually into the soil at application rates of 1%, 3%, and 5% by weight. These application levels were selected for controlled-condition experiments to examine applicatio rate-dependent responses and to enhance treatment contrast for hyperspectral and machine learning analyses, rather than to directly simulate typical field-scale application rates. The biochar-soil mixtures were thoroughly homogenized to ensure even distribution. The amended soils were transferred into plastic pots (8 cm diameter × 5 cm height), each containing 50 g of the prepared mixture. A control group without biochar amendment was

included for comparison. All treatments were prepared in duplicate under identical conditions.

Baseline soil samples were collected prior to biochar amendment to verify initial soil uniformity. Physicochemical properties reported in this study were measured after biochar amendment but before lettuce planting, thereby isolating biochar-induced changes in soil properties from plant–soil interactions. Soil pH (1:1 w/v) and electrical conductivity (1:5 w/v) were measured using calibrated meters. Cation-exchange capacity (CEC) was determined by the 1 M NH_4OAc method (pH 7.0). Water-holding capacity (WHC) was evaluated gravimetrically as $WHC = (W_{sat} - W_{dry})/W_{dry} \times 100\%$ [20]. Additionally, the concentration of polycyclic aromatic hydrocarbons (PAHs) in the biochar-amended soils was analyzed using gas chromatography mass spectrometry (GC-MS, Intuvo GC-MSD/Agilent 7697A, Agilent, Santa Clara, CA), 10 μg of the soil was suspended in 100 μL dichloromethane for the test, and the contents of PAHs were calculated by integrating and comparing with NIST Mass Spectral Library Library [21].

2.3 Lettuce cultivation and performance against water stress

Parris Island Cos lettuce seeds (*Lactuca sativa L.*, provide by The Old Farmer's Almanac, Dublin, NH) were sown directly into the prepared soil mixture (with or without biochar amendment) and cultivated under controlled greenhouse conditions with a 16-hour light/8-hour dark photoperiod, day/night temperatures of 25 ± 2 °C/18 ± 2 °C, and relative humidity maintained at approximately 60% [22]. After germination, seedlings were thinned to two plants per pot.

The pot experiment was conducted over a total duration of 21 days, consisting of a 14-day establishment phase followed by a 7-day reduced-irrigation period to induce water stress. Within 14 days of sowing establishment period (DAS), all pots were irrigated every 4 hours for 10 seconds using an automated drip system delivering water at flow rate of 240 mL/min per emitter, corresponding to 40 mL per irrigation event per pot, to maintain adequate and consistent soil moisture.

At harvest, several morphological and biochemical parameters were evaluated to assess the effects of biochar amendment under water stress conditions. Shoot height and root length were measured manually using a standard ruler. Fresh biomass was recorded immediately after harvesting the above- and below-ground portions of each plant. The moisture content was determined by the halogen moisture analyzer (Torbal BTS110, Scientific Industries, Inc., Bohemia, NY 11716) operated in fast mode, with each measurement taking approximately 120 seconds. The results were automatically calculated and expressed as a percentage of the fresh weight. Samples were then oven-dried at 65 °C for 72 hours or until a constant weight was achieved to determine dry biomass. The nutrient contents (including nitrogen, phosphorus, potassium, and selected micronutrients) were determined from dried, ground plant tissue. Samples were digested using a standard acid digestion method, and elemental concentrations were analyzed using inductively coupled plasma optical emission spectrometry (ICP-OES, Agilent 5110) [20].

Following this period, a water stress treatment was imposed by reducing the irrigation frequency to every 12 hours while maintaining the same watering duration. The control group continued to receive irrigation every 4 hours for 10 seconds to maintain optimal soil moisture. The reduced irrigation schedule was maintained for the remainder of the growth period. Direct measurements of soil moisture content or soil water potential were not conducted during the water-stress period. Plant growth and physiological parameters were monitored throughout the experiment to evaluate the interactive effects of water limitation and biochar application.

2.4 Hyperspectral Imaging (HSI) and Machine Learning Model Training

Hyperspectral images of representative lettuce plants from each treatment group were acquired using a high-resolution near-infrared hyperspectral imaging system. The system consists of a near-infrared (900-1700 nm) pushbroom hyperspectral camera, a linear scanning stage, two 100 W tungsten halogen banks, and the perClass Mira software (MV.C SCAN, Headwall Photonics, Bolton, MA, USA). Integration time was set so the peak digital number was approximately 75% of the maximum value (4096). To achieve square pixels, the scanning speed was automatically calculated by the perClass Mira software using a circular test pattern. Dark current and white reference calibration were performed before plant imaging for reflectance conversion using the internal mechanical shutter and a white reference panel, respectively. Each hyperspectral cube has dimensions of 201 × 760 × 640, corresponding to 201 spectral bands, 760 pixels in height (image lines), and 640 pixels in width (samples per line). In total, 196 image samples were collected [23]. The spectral data were processed to extract reflectance values, which were exported as ENVI files using Python for subsequent analysis. Each dataset was paired with a ground-truth measurement of plant moisture content.

A convolutional neural network (CNN) was developed to predict plant moisture content directly from the hyperspectral data. The model architecture consisted of two convolutional layers followed by two fully connected layers [24]. The first convolutional layer accepted the 201-channel input and applied 32 filters of size 3×3 with padding of 1, followed by a ReLU activation function and a 2×2 max-pooling operation (stride = 2) to reduce spatial dimensions. The second convolutional layer applied 64 filters of size 3×3, again followed by ReLU activation and max-pooling. The resulting feature maps were flattened and passed through a fully connected layer with 256 neurons (ReLU), and finally, a single output neuron produced the predicted moisture value.

Model training was performed using the Adam optimizer with a learning rate of 0.0001 and a weight decay of 1×10^{-5}. The training process was conducted over 70 epochs using a batch size of 4. The CNN model architecture is summarized in Table 1.

Table 1. Architecture of the CNN regression model used for hyperspectral moisture prediction.

Layer Type	Input Shape	Output Shape	Kernel Size	Other Parameters
Conv2D (ReLU)	(201, 760, 640)	(32, 760, 640)	3x3	Padding=1
MaxPooling2D	(32, 760, 640)	(32, 380, 320)	2x2	Stride=2
Conv2D (ReLU)	(32, 380, 320)	(64, 380, 320)	3x3	Padding=1
MaxPooling2D	(64, 380, 320)	(64, 190, 160)	2x2	Stride=2
Fully Connected (ReLU)	(64*, 190,* 160)	256	-	-
Output Layer	256	1	-	-

Model performance was assessed using several regression metrics: Mean Squared Error (MSE), Root Mean Squared Error (RMSE), and Mean Absolute Error (MAE) [25]. These metrics quantify the magnitude of differences between predicted and actual moisture values and the formula were displayed below. Specifically, MSE squares the residuals, making it sensitive to larger errors; RMSE is the square root of MSE and maintains the same unit as the target variable; MAE averages the absolute differences, giving a more balanced view of prediction accuracy. Lower values for all three metrics indicate better model performance.

$$\mathrm{MSE}=\frac{1}{n}\sum_{i}^{n}(y_i-\hat{y}_i)^2 \quad (1)$$

$$\mathrm{RMSE}=\sqrt{\frac{1}{n}\sum_{i=1}^{n}(y_i-\hat{y}_i)^2} \quad (2)$$

$$\mathrm{MAE}=\frac{1}{n}\sum_{i=1}^{n}\left|y_i-\hat{y}_i\right| \quad (3)$$

To assess the presence of systematic bias, two additional metrics were used: *slope* and *bias* [26]. *Slope* was computed as the coefficient of linear regression between predicted and actual values in a scatter plot, and *bias* was calculated as the mean difference between predicted and true values. An ideal model would exhibit a slope close to 1 and bias close to 0, indicating minimal overestimation or underestimation across predictions.

$$\mathrm{Slope}=\frac{\sum_{i=1}^{N}(y_i-E_y)(\hat{y}_i-E_y)}{\sum_{i=1}^{N}(y_i-E_y)^2} \quad (4)$$

$$\mathrm{Bias}=\frac{1}{n}\sum_{i=1}^{n}(\hat{y}_i-y_i)^2 \quad (5)$$

Overall, the HSI–CNN workflow followed a sequential pipeline consisting of hyperspectral image acquisition, reflectance calibration and plant-level data extraction, model training using paired spectral–trait datasets, and performance evaluation against experimentally measured moisture content. Specifically, calibrated hyperspectral cubes were processed to extract reflectance information for each plant sample, which was then used as input to the CNN model for training and prediction. Model outputs were subsequently compared with ground-truth moisture measurements using standard regression metrics (MSE, RMSE, MAE), as well as slope and bias, to assess both prediction accuracy and systematic error.

2.5 Spectral-trait correlation analysis

To support interpretation of hyperspectral features associated with plant water status, correlations between selected spectral regions and measured plant morphological and physiological indicators were examined as a supplementary analysis. Mean reflectance values were extracted from predefined wavelength regions identified in the hyperspectral data and compared with corresponding plant traits, including fresh biomass, plant height, and leaf moisture content.

Pearson's correlation coefficients were calculated to evaluate relationships between spectral features and plant traits. This analysis was conducted to assess consistency between observed spectral-trait associations and previously reported absorption features related to water content, plant structure, and biochemical composition. The spectral-trait correlation analysis was intended to support interpretation of the HSI-CNN model rather than to serve as an independent predictive framework.

2.6 Data analysis

All measurements, including elemental composition, physicochemical properties, volatile compound profiles, and plant physiological data, were conducted in triplicate. Biochar preparation procedures and filtration experiments were also performed in triplicate to ensure reproducibility. Lettuce plants were grown in five independent batches under well-controlled greenhouse conditions to account for potential environmental variability and enhance statistical robustness. Results are presented

as mean ± standard deviation unless otherwise specified.

Statistical analyses were conducted using one-way analysis of variance (ANOVA), followed by post hoc tests to evaluate differences between treatment groups. A significance level of $P < 0.05$ was used to determine statistical significance. Graphical representations of the data were generated using OriginPro 2023 (OriginLab Corporation, Northampton, MA, USA).

3. Results

3.1 Biochar preparation and characterization

The three corn-stalk-derived biochars (CSB350, CSB550, and CSB700) displayed clear temperature-dependent trends in physicochemical properties [27]. As pyrolysis temperature increased from 350 ºC to 550ºC and 700 ºC, yield declined from 41.43% to 28.60% and bulk density decreased from 0.623 to 0.501 g/cm^3, while carbon content rose from 79.32% to 85.89% and H/C ratio dropped from 0.495 to 0.182, indicating greater aromaticity. Structural parameters improved, with BET surface area increasing from 15.42 to 31.70 m^2/g and pore volume from 0.01772 to 0.02793 cm^3/g. CEC also increased from 53.77 to 63.94 cmol(+)/kg, and pH rose from 9.77 to 10.52. These shifts suggest enhanced stability, sorption potential, and water-holding capacity at higher pyrolysis temperatures [28]. Full data are provided in Supplementary Information (Section S1, Table S1).

3.2 Biochar effects on soil water regulation

Biochar amendment induced systematic changes in soil physicochemical properties that are directly relevant to soil water regulation under drought conditions. Rather than serving as a comprehensive soil characterization, this section provides functional context for interpreting subsequent plant growth and water-status responses. The effects of biochar amendment depended on both application rate and pyrolysis temperature (Table 2).

Overall, biochar incorporation reduced soil bulk density and substantially increased soil porosity, surface area, and total pore volume relative to the untreated control. These structural changes were more pronounced at higher application rates and for biochars produced at elevated pyrolysis temperatures (CSB550 and CSB700), reflecting the greater intrinsic porosity and surface functionality of high-temperature biochars. Such modifications are expected to enhance soil water retention and improve root-zone moisture availability during short-term water limitation.

Biochar amendment also increased soil cation exchange capacity (CEC) and moderately elevated soil pH. The enhancement of CEC was particularly evident for high-temperature biochars, indicating improved nutrient buffering capacity that may support plant function under drought stress. In parallel, soil water-holding capacity (WHC) increased consistently across all biochar-amended treatments compared to the untreated soil, with the greatest improvements observed at higher application rates of CSB550 and CSB700. Together, these soil responses indicate that biochar amendment alters the physical and chemical environment of the soil in ways that favor water retention and nutrient availability. These functional changes provide a mechanistic basis for the improved plant water status and growth performance observed under drought conditions, which are discussed in the following sections. Detailed numerical values and statistical comparisons are summarized in Table 2.

PAH analysis of biochar-amended soils showed naphthalene (1.20 to 1.87 mg/kg) and phenanthrene (0.70 to 1.20 mg/kg) as the most abundant compounds, with lower levels of fluorene, fluoranthene, anthracene, benz[a]anthracene, and indeno[1,2,3-cd]pyrene (all < 0.68 mg/kg). High-molecular-weight PAHs were not detected. All values were below regulatory limits, indicating no

toxicity concerns (Table S2). Although low-molecular-weight PAHs such as naphthalene have been reported to influence early plant development at elevated concentrations, the levels detected in this study were substantially lower than reported phytotoxic thresholds, suggesting that PAHs were unlikely to be the primary factor contributing to the observed early germination delay.

Table 2. Physicochemical properties of soils measured after biochar amendment and prior to lettuce planting

Soil type	Density (g/cm^3)	BET surface area (m^2/g)	Total pore volume (cm^3/g)	Cation exchange capacity (cmol(+)/kg)	pH	Water holding capacity (%)
Untreated Soil	1.12 ± 0.05^{a}	3.35 ± 0.05^{a}	0.011 ± 0.001^{a}	6.75 ± 0.05^{a}	6.30 ± 0.04^{a}	28.5 ± 0.2^{a}
Soil + CSB350_1 wt%	1.10 ± 0.05a	4.23 ± 0.04^{b}	0.023 ± 0.001^{b}	8.52 ± 0.08^{b}	6.52 ± 0.03^{b}	33.7 ± 0.3^{b}
Soil + CSB350_3 wt%	1.08 ± 0.02^{ab}	4.43 ± 0.05^{b}	0.034 ± 0.003^{c}	9.62 ± 0.07^{c}	6.71 ± 0.05^{c}	34.1 ± 0.2^{bc}
Soil + CSB350_5 wt%	1.07 ± 0.04^{ab}	4.82 ± 0.05^{c}	0.057 ± 0.004^{d}	10.07 ± 0.11^{d}	6.68 ± 0.04^{cd}	34.6 ± 0.2^{c}
Soil + CSB550_1 wt%	1.11 ± 0.04^{a}	4.66 ± 0.03^{bc}	0.157 ± 0.009^{e}	11.77 ± 0.09^{c}	6.64 ± 0.03^{d}	34.3 ± 0.4^{bc}
Soil + CSB550_3 wt%	1.08 ± 0.05^{a}	5.20 ± 0.04^{d}	0.182 ± 0.002^{f}	12.22 ± 0.21^{e}	6.73 ± 0.04^{c}	34.8 ± 0.3^{c}
Soil + CSB550_5 wt%	1.06 ± 0.03^{ab}	5.77 ± 0.04^{e}	0.191 ± 0.004^{g}	14.78 ± 0.12^{f}	6.75 ± 0.05^{ce}	35.9 ± 0.5^{d}
Soil + CSB700_1 wt%	1.09 ± 0.04^{ab}	4.66 ± 0.03^{b}	0.158 ± 0.001^{e}	12.95 ± 0.13^{c}	6.62 ± 0.02^{d}	34.4 ± 0.2^{c}
Soil + CSB700_3 wt%	1.07 ± 0.02^{ab}	5.34 ± 0.04^{d}	0.188 ± 0.002^{f}	16.34 ± 0.16^{d}	6.76 ± 0.04^{e}	34.9 ± 0.1^{c}
Soil + CSB700_5 wt%	1.05 ± 0.02^{b}	5.80 ± 0.04^{e}	0.193 ± 0.003^{g}	17.22 ± 0.12^{g}	6.77 ± 0.05^{e}	35.6 ± 0.2^{d}

*The results were presented as mean ± SD on dry basis, where n = 9. Tukey's HSD test was used to determine the statistical difference ($p<0.05$). The mean value accompanied by the same letter indicates no significant differences among all samples in the same column.

3.3. Plant growth and response to water stress

To evaluate the role of biochar in enhancing drought resilience under limited watering condition, lettuce was cultivated under two irrigation regimes: well-watered and water-stressed. The first 14 days after sowing were designed to support initial establishment under regular watering, allowing plants to develop in untreated or biochar-amended soils. During this phase, we also assessed how biochar type and application rate influenced early growth. On 14 days after sowing, a 7-day water-stress period was initiated for half of the plants to simulate drought conditions, while the remaining plants continued under full irrigation. Plant performance was monitored through morphological metrics, leaf moisture content, and hyperspectral imaging to determine the effectiveness of biochar in mitigating water stress.

During the initial 14 days after sowing period under adequate watering, all treatments achieved successful germination, with no significant differences observed between the control and biochar-amended soils (71-74%, Table 3). This suggests that biochar did not impair seed viability under favorable moisture conditions. However, a consistent delay in seedling emergence was observed in biochar-amended soils compared to the control (Figure 1). In the untreated soil, shoots began to emerge on 3 days after sowing (0.36 cm), while no emergence was recorded in any biochar treatments at that time. By 4 days after sowing, all biochar treatments exhibited shoot emergence (0.35-0.56 cm), indicating a uniform delay of approximately one day. Among them, CSB550_5 wt% showed the most advanced emergence (0.56 cm), suggesting that higher pyrolysis temperature and application rate may partially alleviate this delay. Despite this initial lag, seedlings in biochar-treated soils exhibited accelerated growth in the following days. By 6 days after sowing, shoot lengths in all biochar treatments (2.94 to 3.70 cm) exceeded those in the control (2.83 cm), and this advantage persisted throughout the period. Higher pyrolysis temperatures and amendment rates-particularly with CSB550 and CSB700-consistently supported greater shoot elongation. On 10 days after sowing, control seedlings reached 5.46 cm, while CSB700_5 wt% and CSB550_5 wt% treatments achieved 7.76 cm and 7.53 cm, respectively. By 14 days after sowing, shoot lengths ranged from 7.22 cm (CSB350_1 wt%) to 8.72 cm (CSB700_5 wt%) in biochar treatments, compared to 6.12 cm in the control. These findings highlight the influence of both biochar type and application rate on early vegetative growth.

By 14 days after sowing, the extent of growth improvement observed among treatments varied depending on the biochar type (i.e., pyrolysis temperature) and its usage amount (Table 3 and Figure 2). In the control group, root and shoot lengths averaged 6.01 cm and 6.12 cm, respectively. Application of CSB350 biochar led to moderate improvements, with the highest values observed at 5 wt% (6.97 cm root, 7.63 cm shoot). CSB550 treatments produced further increases, reaching 7.27 cm root and 8.62 cm shoot at 5 wt%. On the CSB700 group, while the shoot length (8.72 cm at 5 wt%) was not significantly higher than that of CSB550, CSB700 demonstrated a stronger effect on root elongation, with root length reaching 8.15 cm. The other investigations also confirmed the benefits of biochars. The fresh yields of lettuce increased progressively with both biochar application rate and pyrolysis temperature. Compared to the control (2.23g), the yield significantly improved under CSB350 and CSB550 treatments, reaching up to 2.43 g in the CSB550_5 wt% group and 2.44 g in the CSB700_5 wt% group. Moisture content also increased with biochar addition, from 91.12% in the control to a maximum of 93.12% in the CSB700_5 wt% treatment. These results suggested that biochar amendments, particularly those produced at higher pyrolysis temperatures (CSB550 and CSB700), effectively improve biomass accumulation and water retention capacity in lettuce under limited moisture conditions.

Table 3. Lettuce performance with biochar amendments on 14 days after sowing under normal irrigation

Plant growing settings	Germination rate/%	Yield (fresh weight)/g	Leaf moisture content/%
Untreated Soil	71.00 ± 7.38	5.19 ± 0.05^{a}	90.12 ± 0.35^{a}
Soil + CSB350_1 wt%	72.00 ± 7.89	5.30 ± 0.04^{b}	90.87 ± 0.26^{b}
Soil + CSB350_3 wt%	71.00 ± 7.38	5.35 ± 0.04^{b}	90.99 ± 0.29^{b}
Soil + CSB350_5 wt%	73.00 ± 6.75	5.38 ± 0.06^{b}	91.15 ± 0.31^{b}
Soil + CSB550_1 wt%	74.00 ± 5.16	5.39 ± 0.07^{b}	91.23 ± 0.22^{b}
Soil + CSB550_3 wt%	72.00 ± 6.32	5.42 ± 0.05^{b}	91.77 ± 0.29^{bc}
Soil + CSB550_5 wt%	72.00 ± 7.88	5.43 ± 0.06^{bc}	92.06 ± 0.25^{c}
Soil + CSB700_1 wt%	71.00 ± 8.76	5.47 ± 0.04^{bc}	91.89 ± 0.17^{c}
Soil + CSB700_3 wt%	73.00 ± 4.83	5.49 ± 0.04^{bc}	92.09 ± 0.23^{c}
Soil + CSB700_5 wt%	72.00 ± 4.22	5.52 ± 0.05^{c}	92.12 ± 0.26^{c}

The results of germination rates were presented as mean ± SD, where n=10. The yields and moisture contents were presented as mean ± SD, where n=6. Tukey's HSD test was used to determine the statistical difference ($p<0.05$). The mean values labeled by the same letter indicate no significant differences within the same column.

With 14 days after sowing of regular irrigation, all plants were well established. To assess the role of biochar in mitigating drought stress, the treatments were divided into two groups to assess the role of biochar in drought mitigation. One group continued to receive regular watering for the full 21-day period, while the other underwent 7 days of water reduction (i.e., 14 days of regular watering followed by 7 days of limited irrigation). Plant performance under these two regimes was monitored using hyperspectral imaging, leaf moisture content measurements, and final harvest data to evaluate biochar's effectiveness in supporting plant resilience under water-limited conditions.

During the 7-day water-stress period, hyperspectral imaging (Figure S1) revealed pronounced differences in plant responses across treatments. In the untreated control group under reduced watering, lettuce plants began to collapse visibly, with shoots falling over and leaves exhibiting clear signs of withering by 21 days after sowing, indicating severe drought stress. In contrast, plants grown in biochar-amended soils maintained upright shoot structure and firm, turgid leaves throughout the stress phase, suggesting improved resilience to water limitation.

Leaf moisture content was monitored throughout the 7-day water-stress period to assess plant hydration dynamics (Figure 3). All treatments showed declining trends between 14 days after sowing and 21 days after sowing, but with significant differences in rate and final values. The untreated control had the steepest decline, dropping from 91.47% to 88.72% by 21 days after sowing. In contrast, CSB350 treatments showed only moderate improvements, with final moisture content ranging from 89.92% (1 wt%) to 90.01% (5 wt%). No clear application rate-dependent trend was observed. CSB550 showed a stronger protective effect, with a clear application rate-response: leaf moisture increased from 90.34% at 1 wt% to 91.08% at 5 wt%. CSB700 treatments also consistently outperformed the control, with final values ranging from 90.82% (1 wt%) to 91.05% (5 wt%). Compared to the control, which lost nearly 2.8 percentage points over 7 days, the highest-performing biochar treatments (CSB550 and CSB700 at 5 wt%) retained > 91% moisture, and among the treatments evaluated, CSB700 applied at 5 wt% resulted in the highest soil water-holding capacity and leaf moisture content under water-limited

conditions. These results suggest that both higher pyrolysis temperatures and greater application rates enhance the effectiveness of biochar in mitigating drought-induced water loss in lettuce.

To further evaluate the drought-mitigating potential of biochar, lettuce performance was compared between plants maintained under full watering and those subjected to 7 days of reduced irrigation after the initial 14 days after sowing establishment phase (Table 4). In the control group, drought stress caused marked reductions in all growth parameters: fresh weight dropped from 7.66 g to 6.31 g, height from 18.22 cm to 13.37 cm, and moisture content from 90.37% to 85.47%. Biochar-amended soils alleviated these declines in a type- and application rate-dependent manner. Under reduced watering, CSB350 showed moderate effects: fresh weight ranged from 7.38 g at 1 wt% to 7.75 g at 5 wt%, height from 16.22 cm to 17.09 cm, and moisture from 89.74% to 90.01%. CSB550 produced stronger improvements, with fresh weight increasing from 8.02 g (1 wt%) to 8.33 g (5 wt%), height from 17.22 cm to 17.35 cm, and moisture from 90.06% to 90.84%. CSB700 performed similarly or slightly better, with fresh weights of 8.20 g (1 wt%) to 8.40 g (5 wt%), heights of 17.18 cm to 17.35 cm, and moisture contents from 90.78% to the highest recorded value of 91.10%. These results demonstrate that higher pyrolysis temperatures (550 and 700 °C) and higher application rates (3 and 5 wt%) consistently supported greater biomass, plant height, and water retention compared to both the control and lower-temperature biochar. These findings indicate that biochar efficacy under drought conditions is strongly influenced by both material properties and application rate, with higher-pyrolyzed biochars applied at ≥3 wt% offering the greatest protection for plant growth and water status.

Table 4. Lettuce growth and water status under varying irrigation and biochar treatments

Soil type	Irrigation	Fresh weight/g	Total height/cm	Plant moisture/%*
Untreated Soil	21 days of regular watering	7.66 ± 0.05	18.22 ± 0.07	90.37 ± 0.33
	14 days of regular watering and 7 days of reduced watering	6.31 ± 0.04	13.37 ± 0.04	85.47 ± 1.10
Soil + CSB350_1 wt%	21 days of regular watering	7.79 ± 0.04	18.25 ± 0.05	92.17 ± 0.24
	14 days of regular watering and 7 days of reduced watering	7.38 ± 0.06	16.22 ± 0.04	89.74 ± 0.23
Soil + CSB350_3 wt%	21 days of regular watering	7.94 ± 0.05	18.28 ± 0.06	92.67 ± 0.32
	14 days of regular watering and 7 days of reduced watering	7.62 ± 0.05	16.38 ± 0.02	89.86 ± 0.48
Soil + CSB350_5 wt%	21 days of regular watering	8.02 ± 0.06	18.22 ± 0.05	92.76 ± 0.35
	14 days of regular watering and 7 days of reduced watering	7.75 ± 0.03	17.09 ± 0.03	90.01 ± 0.32
Soil + CSB550_1 wt%	21 days of regular watering	8.23 ± 0.05	18.32 ± 0.05	92.33 ± 0.37
	14 days of regular watering and 7 days of reduced watering	8.02 ± 0.04	17.22 ± 0.05	90.06 ± 0.22
Soil +	21 days of regular watering	8.38 ± 0.03	18.46 ± 0.07	92.36 ± 0.47

CSB550_3 wt%	14 days of regular watering and 7 days of reduced watering	8.20 ± 0.04	17.35 ± 0.03	90.67 ± 0.29
Soil + CSB550_5 wt%	21 days of regular watering	8.45 ± 0.06	18.48 ± 0.03	92.75 ± 0.39
	14 days of regular watering and 7 days of reduced watering	8.33 ± 0.03	17.29 ± 0.04	90.84 ± 0.42
Soil + CSB700_1 wt%	21 days of regular watering	8.33 ± 0.04	18.29 ± 0.05	92.79 ± 0.33
	14 days of regular watering and 7 days of reduced watering	8.20 ± 0.05	17.18 ± 0.03	90.78 ± 0.31
Soil + CSB700_3 wt%	21 days of regular watering	8.49 ± 0.07	18.34 ± 0.06	93.22 ± 0.21
	14 days of regular watering and 7 days of reduced watering	8.39 ± 0.04	17.23 ± 0.04	91.05 ± 0.19
Soil + CSB700_5 wt%	21 days of regular watering	8.48 ± 0.05	18.52 ± 0.04	93.34 ± 0.25
	14 days of regular watering and 7 days of reduced watering	8.40 ± 0.03	17.35 ± 0.05	91.10 ± 0.18

The results of germination rates were presented as mean ± SD, where n=10. The yields and moisture contents were presented as mean ± SD, where n=6.

3.4 Integrated Hyperspectral and Experimental Assessment

Hyperspectral imaging was employed to capture treatment-specific differences in plant physiological status under both regular and water-limited conditions. Average reflectance spectra revealed distinct spectral patterns among treatments, with biochar-amended plants exhibiting clear differences relative to the water-stressed control across multiple wavelength regions (Figure 4).

To support interpretation of these spectral patterns, relationships between selected spectral regions (908-970, 1120-1160, 1275-1325, 1416-1470, and 1630-1680 nm) and plant morphological and physiological indicators were examined. The wavelength regions (presented in S3 in supplementary materials) were selected based on previously reported absorption features associated with plant water status, nitrogen-related compounds, and structural carbohydrates in the near- and shortwave-infrared regions. Rather than detailing wavelength-specific interpretations in the main text, these analyses are summarized here and presented in full in the Supplementary Material. Overall, spectral variations observed in biochar-amended plants were consistent with experimentally measured differences in plant growth and water status.

Principal component analysis (PCA) was used to evaluate multivariate spectral responses across biochar type, application rate, and watering regime (Figures 5-6). The first two principal components explained 99.6% of the total spectral variance (Figure 5). PC1 primarily differentiated samples by biochar type and application rate, while PC2 separated samples by watering regime. Under drought conditions, biochar-amended plants clustered more closely with regularly watered treatments than with the water-stressed control, indicating mitigation of drought-associated spectral shifts.

Analysis of PC1 score distributions (Figure 6) further demonstrated application rate-dependent effects, particularly for CSB550 treatments, where increasing biochar application resulted in systematic

shifts in spectral signatures. These results confirm that both biochar properties and application rate strongly influence plant spectral responses under water-limited conditions.

To support interpretation of the observed hyperspectral patterns, relationships between selected spectral regions and measured plant morphological and physiological traits were examined. These spectral-trait correlations were used as an interpretive assessment to evaluate consistency between hyperspectral features and experimentally measured plant responses. Detailed correlation results and wavelength-specific interpretations are provided in the Supplementary Material (Supplementary Section S3 and Table S6).

3.5 Model Performance Evaluation

A convolutional neural network (CNN) was trained using raw hyperspectral data extracted from lettuce images to predict leaf moisture content in a non-destructive manner. Model performance was evaluated using separate training and test datasets, with results summarized in Table 5. The model achieved low prediction errors for both datasets, with mean squared error (MSE), root mean squared error (RMSE), and mean absolute error (MAE) values of 0.0153, 0.1237, and 0.1027 for the training set, and 0.0440, 0.2098, and 0.1678 for the test set, respectively. The MAE for the test dataset corresponds to approximately 1.41% of the observed leaf moisture range (82.15-94.08%).

Predicted moisture values showed strong agreement with measured values, as indicated by a regression slope of 0.97 and a bias of −0.013 (Figure 7). Each data point in Figure 7 represents an individual hyperspectral image paired with its corresponding measured leaf moisture content. Most data points clustered closely around the 1:1 line, indicating minimal systematic over- or underestimation across the range of observations.

At the treatment level, the CNN predictions reflected trends observed in experimental measurements, with biochar-amended treatments generally associated with higher predicted and measured leaf moisture contents under drought conditions compared to the water-stressed control. This consistency indicates that the model captured treatment-related differences in plant water status present in the experimental system.

It should be noted that model training and testing were conducted using data derived from the same controlled experimental setup. Therefore, the reported performance reflects system-specific relationships between hyperspectral signatures and leaf moisture content. Evaluation of model robustness across different crop species, soil types, or environmental conditions is an important direction for future work.

While the CNN model performance was evaluated independently using regression metrics, supplementary spectral-trait correlation analysis was conducted to support interpretation of the hyperspectral features used by the model and is presented in Supplementary Section S3.

Table 5. Performance Metrics for Train and Test Sets

	MSE ($\%^2$)	RMSE (%)	MAE (%)
Train	0.0153	0.1237	0.1027
Test	0.0440	0.2098	0.1678

4. Discussion

4.1 Effects of Biochar Amendment on Soil Moisture and Plant Water Status

Biochar serves as a climate-smart and sustainable soil amendment agent that improves soil fertility, water retention, and plant stress tolerance, while contributing to long-term carbon sequestration[36]. Its porous structure and chemical properties enhance both physical and chemical soil characteristics, particularly under water-limited conditions [37]. A key advantage of biochar is its tunability, with properties adjustable through feedstock and pyrolysis temperature [38]. In this study, we used corn stalk as the feedstock due to its high lignocellulosic content, agricultural abundance, and low cost, making it a practical, eco-friendly option for circular bioeconomy applications. Biochar samples were produced at 350°C, 550°C, and 700°C to assess how pyrolysis temperature influences biochar properties and their effects on soil performance and lettuce growth under varying irrigation regimes.

The results indicated that biochar pyrolysis temperature is a critical factor influencing the physical and chemical properties of corn stalk biochar, which in turn affects its efficacy as a soil amendment. Increasing the pyrolysis temperature from 350°C to 700°C significantly enhanced key biochar properties: carbon content rose from 79.32% (CSB350) to 85.89% (CSB700), while volatile elements such as hydrogen and oxygen decreased. This increase in carbon content is due to the greater thermal decomposition of cellulose, hemicellulose, and lignin at higher temperatures, which drives off volatile compounds, leaving behind a more stable, carbon-rich aromatic matrix [39]. Higher pyrolysis temperatures also promoted larger specific surface areas and greater pore volumes, as the expansion of internal channels and collapse of cell walls during volatile matter expulsion resulted in enhanced microporous and mesoporous structures [40]. Additionally, biochars produced at elevated temperatures showed significant improvements in cation exchange capacity (CEC), increasing from 53.77 cmol(+)/kg in CSB350 to 60.05 cmol(+)/kg in CSB550 and 63.94 cmol(+)/kg in CSB700. This increase in CEC is largely due to the development of aromatic carbon structures and oxygen-containing functional groups (e.g., carboxyl and phenolic groups), which serve as active sites for ion exchange [41]. The formation of micro- and mesopores further enhances CEC by increasing the surface area and pore volume, providing more space for nutrient retention and exchange [41]. These combined chemical and physical enhancements create a favorable matrix for nutrient retention, particularly in degraded or sandy soils, thereby improving soil performance and supporting plant growth under water-limited conditions.

Biochar application significantly altered the physicochemical properties of soil, with marked improvements in porosity, CEC, and WHC. These enhancements were especially prominent with biochars produced at higher pyrolysis temperatures (CSB550 and CSB700) and at higher application rates. The total pore volume increased substantially due to the highly porous structure of highly-pyrolyzed biochars, which introduced additional pore networks into the soil matrix [42]. This enhanced porosity played a critical role in improving WHC, with the capacity rising from 28.5% in untreated soil to 35.6% in soil amended with 5 wt% CSB700. Such an improvement indicates that biochar-amended soils can retain moisture more effectively, a key benefit in regions prone to water scarcity or drought stress. The greater pore volume and surface area of CSB550 and CSB700 likely enhanced root-zone water retention, directly contributing to the higher leaf moisture content observed under drought conditions. In parallel, CEC increased markedly, from 6.75 cmol(+)/kg in untreated soil to 18.22 cmol(+)/kg with 5 wt% CSB700. This improvement is largely attributed to the greater density of oxygen-containing functional groups and mineral-associated sites on highly-pyrolyzed biochars, which are crucial for retaining essential nutrients and promoting soil fertility [43]. Enhanced nutrient retention is particularly valuable for sustainable soil management, as it helps to reduce nutrient leaching and improve plant nutrient uptake. Collectively, these findings underscore the dual role of

biochar as both a physical soil conditioner and a chemical enhancer. In addition to improvements in soil physical properties, biochar amendment—particularly at higher pyrolysis temperatures and application rates—also resulted in significant increases in soil pH. Soil pH is a key regulator of nutrient solubility, ion exchange processes, and root physiological activity, and moderate pH elevation can enhance the availability and uptake of essential nutrients. Accordingly, the observed improvements in soil performance and subsequent plant responses in biochar-amended treatments likely reflect the combined influence of enhanced soil water-holding capacity and pH-mediated chemical effects, rather than a single dominant mechanism. Because these physical and chemical factors act concurrently under the experimental conditions evaluated, their individual contributions were not isolated in the present study. This makes biochar a valuable tool for sustainable agricultural practices, especially in areas facing soil degradation, nutrient depletion, and water stress. By integrating biochar into soil management strategies, we can promote long-term soil health, improve crop resilience to environmental stress, and contribute to climate change mitigation through carbon sequestration. It should be noted that the biochar application rates used in this study correspond to relatively high field-equivalent dosages. The present work was designed as a mechanistic investigation under controlled conditions, and did not evaluate the economic or logistical feasibility of large-scale field deployment. Future studies should assess lower, agronomically realistic application rates under field conditions to translate these findings into practical recommendations.

Increased cation exchange capacity (CEC) in soils amended with higher-pyrolyzed biochars may also contribute to improved nutrient retention under drought conditions by reducing nutrient leaching and maintaining ion availability in the root zone. Although plant tissue nutrient uptake was not directly measured in this study, the observed improvements in plant growth and water status are consistent with enhanced nutrient accessibility mediated by higher soil CEC, as reported in previous studies. Future work incorporating plant nutrient analysis would be valuable for directly linking biochar-induced changes in soil CEC to nutrient uptake dynamics under water stress.

Biochar amendment slightly increased certain PAH concentrations in soil, but levels remained low and within acceptable environmental limits [44]. Naphthalene and phenanthrene were the most frequently detected, likely due to their low molecular weights and high volatility, promoting their formation and persistence during pyrolysis. In contrast, heavier PAHs (e.g., benzo[a]pyrene, indeno[1,2,3-cd]pyrene) were undetected or present only in trace amounts in some treatments (e.g., 5 wt% CSB350 or CSB550). These results indicate that biochar can improve soil properties while keeping PAH levels well below safety thresholds, supporting its use as a sustainable, low-risk amendment when production and application are controlled [44].

The impact of biochar on plant growth is complex, with both short-term inhibitory effects and long-term benefits. This is largely due to biochar's unique features, such as its porous structure, high surface area, and nutrient-holding capacity, which can enhance soil fertility and water retention over time. All treatments exhibited the same levels of germination rate, indicating that biochar did not adversely affect seed viability or the initial stages of germination. The observed differences in growth were therefore not due to variations in germination success.

Biochar amendment initially caused a slight delay in seedling emergence, particularly in soils treated with low-temperature biochar (CSB350) at higher application rates (3-5 wt%). This delay is a well-documented phenomenon in biochar research, with several factors likely contributing. First, biochar's pH and salinity can alter soil conditions, potentially inhibiting seedling germination[45]. The high pH often observed with biochar can affect nutrient availability, while increased salinity may lead

to osmotic stress, making it harder for seeds to establish. Additionally, low-temperature biochars, such as CSB350, contain higher levels of volatile organic compounds and light PAHs, which are phytotoxic to emerging seedlings [46]. Moreover, the porous structure of biochar can hold water and nutrients, which would otherwise be delivered to the seeds, further contributing to a less favorable microenvironment for germination [47]. However, once seedlings emerged, plant growth accelerated significantly, particularly in soils amended with CSB550 and CSB700. This suggests that the initial delay was transient and outweighed by the long-term improvements in soil structure, porosity, and water retention. The enhanced soil properties created a more favorable environment for root development, nutrient uptake, and overall plant growth, particularly under water-limited conditions. These findings highlight the balance between the short-term inhibitory effects of biochar and the long-term benefits it provides for plant growth.

On 14 days after sowing, the effects of biochar amendments on lettuce growth were clearly evident in both shoot and root development. Biochar's porous structure and nutrient-holding capacity likely provided a favorable microenvironment for seedling establishment. Plants grown in biochar-amended soils, especially those treated with higher-pyrolyzed biochars (CSB550 and CSB700), exhibited significantly increased root and shoot growth compared to untreated soils. For example, root growth in soils amended with 5 wt% CSB700 reached 8.15 cm, compared to 6.01 cm in untreated soil. Similarly, shoot growth increased to 8.72 cm in the 5 wt% CSB700 treatment, compared to 6.12 cm in untreated soil. Other biochar treatments, such as CSB550, also showed marked improvements in both root and shoot length, with CSB550 at 5 wt% yielding 7.27 cm for roots and 8.62 cm for shoots, both significantly higher than the untreated soil. In addition to increased growth, biochar-amended soils showed enhanced leaf moisture content. For instance, the moisture content in the 5 wt% CSB700 treatment was 92.12%, compared to 90.12% in untreated soil, further emphasizing biochar's role in improving water retention and overall plant health. These results highlight biochar’s potential to improve early-stage plant growth under the experimental conditions evaluated. The effects were especially pronounced in soils amended with higher-pyrolyzed biochars, suggesting that the physical and chemical properties of biochar are key to its effectiveness in promoting plant growth.

Under water-limited conditions, biochar amendments significantly improved plant performance relative to untreated soils. In this study, improved drought-related performance primarily reflects drought avoidance mechanisms discussed above, rather than intrinsic physiological drought tolerance. This effect was confirmed by both experimental studies and advanced analyses using hyperspectral imaging and convolutional neural network (CNN) modeling.

During the 7-day water-stress period, hyperspectral imaging revealed significant differences in plant responses across treatments, supporting the hypothesis that biochar amendments improve drought resilience. In the untreated control group, lettuce plants showed visible signs of collapse, with shoots falling over and leaves wilting by 21 days after sowing, indicative of severe drought stress. In contrast, plants grown in biochar-amended soils, particularly those treated with higher pyrolysis temperature biochars (CSB550 and CSB700), exhibited improved resilience, maintaining upright shoot structures and turgid leaves throughout the stress phase. These visual differences were supported by the leaf moisture content data shown in Figure 3, where biochar treatments consistently retained more moisture than the untreated control over the 7-day stress period. Although statistically significant differences in leaf moisture content were observed among treatments, the absolute magnitude of these changes was relatively small. These differences are therefore interpreted as indicators of relative plant hydration status under identical irrigation regimes rather than as direct measures of physiological performance or

yield formation. Under short-term water stress and early growth conditions, modest shifts in tissue water content may nonetheless influence the timing and progression of stress responses; however, the present study does not establish thresholds for physiological or agronomic relevance. Accordingly, the observed moisture differences are discussed in a comparative context, and extrapolation to yield or long-term performance is avoided. It should be noted that this study was conducted as a short-term (21-day) pot experiment using small containers under controlled greenhouse conditions. While this experimental design enables isolation of biochar-induced effects and minimizes environmental variability, it inherently constrains root development and simplifies soil–plant–atmosphere interactions compared with field conditions. As a result, the magnitude of biochar-related improvements in soil water retention and early plant performance under water stress may be accentuated relative to longer-term or field-scale systems. Accordingly, the observed responses should be interpreted as short-term, controlled-condition effects rather than direct predictions of long-term persistence or agronomic performance. Because direct measurements of soil moisture content or soil water potential were not collected during the stress period, drought intensity was evaluated indirectly through relative comparisons of plant water status and performance under an identical irrigation regime across treatments. Further studies incorporating extended growth durations, field-based trials, and direct measurements of soil moisture or water potential are needed to evaluate the scalability and durability of these effects.

The untreated control showed a sharp decline in moisture content, dropping from 91.47% at Day 0 to 88.72% by 7 days after sowing, indicating significant water loss under drought stress. In contrast, biochar-amended soils exhibited more gradual reductions in moisture content. CSB350 treatments showed moderate improvements, with final values ranging from 89.92% (1 wt%) to 90.01% (5 wt%), without a clear application rate-dependent trend. However, higher-pyrolyzed biochars (CSB550 and CSB700) demonstrated stronger protective effects, with moisture content ranging from 90.34% to 91.08% in CSB550 treatments and 90.82% to 91.16% in CSB700 treatments by 7 days after sowing. These trends are consistent with the soil physical modifications induced by higher-pyrolyzed biochars discussed above. Additionally, the application rate of biochar applied had a significant impact on moisture retention, with higher application rates (3-5 wt%) showing enhanced water retention compared to lower application rates [48]. For example, CSB550 at 5 wt% and CSB700 at 5 wt% consistently retained the highest moisture, reinforcing the importance of both the biochar's properties and its application rate in mitigating water loss during drought stress.

In sum, higher-pyrolyzed biochars, particularly at higher application rates, exhibited more pronounced effects on moisture-related traits, likely due to enhanced porosity and surface area. These observations reflect the experimental conditions evaluated in this study and do not imply a universally optimal biochar type or application rate. These findings underscore the potential of biochar, particularly those produced at higher pyrolysis temperatures and applied at optimal application rates, to enhance early-stage plant performance under water-limited conditions [49]. By enhancing soil structure and moisture retention under controlled conditions, biochar demonstrates promise as a strategy for mitigating drought-induced stress, warranting further evaluation under field-relevant scenarios.

4.2 Hyperspectral-ML Interpretation of Plant Moisture and Physiological Traits

Building on the experimental results, hyperspectral imaging provided a rapid, non-destructive means of capturing treatment-specific differences in leaf hydration, structural biomass, and biochemical composition under both regular and drought conditions. The spectral patterns observed in

water-, nitrogen-, and structural carbohydrate-sensitive wavelength regions closely paralleled measured trends in fresh biomass, leaf moisture content, and nutrient accumulation, confirming that HSI reliably reflected the physiological responses induced by biochar amendments. This consistency not only validates the spectral approach but also highlights its capacity to detect subtle biochemical and structural shifts that may precede visible symptoms of drought stress.

In addition to hyperspectral imaging, a range of techniques has been widely used to characterize crop morphological and physiological indicators, including destructive gravimetric measurements, gas exchange analysis, chlorophyll fluorescence, thermal imaging, and RGB-based digital phenotyping [44]. While these approaches provide valuable trait-specific information, they often capture a limited set of indicators, require physical sampling, or are sensitive to environmental conditions, making them less suitable for continuous or high-throughput monitoring under dynamic stress scenarios.

Compared with these methods, hyperspectral imaging offers distinct advantages by simultaneously capturing spectral information related to plant water status, biochemical composition, and structural characteristics across hundreds of contiguous wavelengths. This enables the detection of subtle physiological changes induced by biochar amendment and drought stress that may not be visually apparent or detectable using single-sensor approaches. In the context of this study, the non-destructive and high-throughput nature of hyperspectral imaging was particularly advantageous for tracking treatment-specific moisture dynamics over time.

When coupled with a convolutional neural network (CNN) predictive model, HSI advanced from a diagnostic tool to a data-driven predictive framework within the experimental system evaluated. The integrated HSI–CNN framework achieved high predictive accuracy for leaf moisture content (MAE = 0.17, RMSE = 0.21), with model outputs closely matching experimental measurements, including the highest recorded value of 91.10% in CSB700 (5 wt%) under drought conditions. This level of prediction error is substantially smaller than typical biological variability and measurement uncertainty associated with destructive moisture assessments, indicating that the model reliably captured relative differences in plant hydration under identical irrigation regimes. Consistent with this performance, the CNN model showed strong agreement between predicted and measured leaf moisture values on the test dataset, indicating its ability to capture relative differences in plant hydration under identical growth conditions.Together, these results demonstrate the model's capacity to translate high-dimensional spectral features into quantitative physiological metrics.

Although the CNN model demonstrated high predictive accuracy for leaf moisture content within this study, it is important to note that model training and testing were conducted using data derived from a single experimental system, including the same crop species, soil type, controlled growth environment, and hyperspectral imaging configuration. As such, the observed model performance primarily reflects within-system predictive capability rather than broad transferability across diverse agronomic conditions. The CNN framework presented here is therefore intended as a proof-of-concept for integrating hyperspectral imaging with data-driven modeling to capture plant water status under controlled conditions. Future work incorporating external validation datasets spanning different crops, soils, environmental conditions, and imaging setups will be necessary to assess model robustness and generalizability.

Within this defined experimental scope, the HSI–CNN framework nonetheless offers important practical advantages. By enabling real-time, non-invasive, and high-throughput assessment of plant water status, the integrated HSI–CNN approach overcomes key limitations of traditional destructive measurement techniques. The ability to simultaneously quantify hydration alongside structural and

biochemical traits makes this framework particularly well suited for evaluating biochar-mediated drought responses, optimizing amendment strategies, and supporting data-driven crop management decisions in water-limited agricultural systems [50]. As such, hyperspectral imaging, when combined with machine learning, serves as a complementary and effective tool for interpreting plant physiological responses under drought stress rather than a replacement for conventional experimental measurements.

4.3 Implications for Precision Agriculture and Sustainable Drought Management

Our integrated HSI-CNN model demonstrated strong predictive accuracy for lettuce moisture content, achieving a test Mean Absolute Error (MAE) of 0.17 and Root Mean Squared Error (RMSE) of 0.21, reflecting precise moisture estimation. The model's predictions closely mirrored measured physiological data, showing a consistent trend of increased moisture retention in biochar-amended plants under drought stress. For instance, the leaf moisture content in the CSB700 5 wt% treatment reached 91.10%, which was accurately predicted by the model. This strong correlation confirms that the HSI-CNN model can reliably capture plant responses, offering a non-invasive alternative that complements traditional destructive measurements. Such a method provides not only accuracy but also the flexibility to monitor plant health at a much larger scale and frequency than traditional approaches.

The integration of hyperspectral imaging and CNN also opens new opportunities for precision agriculture. By enabling non-destructive, high-throughput monitoring of plant water status, this approach could revolutionize irrigation management [51]. It can allow farmers to precisely tailor water applications to the actual needs of the plants, optimizing water usage and reducing waste. In regions facing water scarcity, this could be a critical tool for enhancing crop resilience and improving water use efficiency, which are essential for sustainable farming practices [52]. For researchers, this technology offers a scalable method to assess physiological responses across large plant populations. It accelerates studies on soil amendments, plant breeding, and stress tolerance to water limitation by enabling real-time monitoring without the need for destructive sampling, thus facilitating more rapid data collection and analysis. The ability to monitor changes in plant health with fine spatial and temporal resolution also supports the development of predictive models for plant growth under various environmental conditions.

Beyond water management, the integration of HSI-CNN modeling can be applied to a wide range of plant health assessments, such as detecting nutrient deficiencies, disease monitoring, and overall plant stress. The high-dimensional data captured by hyperspectral imaging, combined with the predictive power of CNNs, offers unprecedented insights into plant physiology, making it a valuable tool for advancing agricultural research and optimizing crop management.

Ultimately, this technology-driven approach can reduce labor costs, increase data accuracy, and enhance our understanding of plant responses to environmental stressors. It holds significant promise in improving the development of sustainable farming practices that are adaptive to changing climate conditions, offering farmers and researchers a sophisticated tool for dynamic decision-making in the face of global challenges.

5. Conclusion

This study demonstrates two complementary advances toward climate-resilient precision agriculture. First, corn-stalk-derived biochars produced at higher pyrolysis temperatures, particularly when applied at ≥3 wt%, enhanced soil water-holding capacity and supported improved plant hydration

and early-stage growth under short-term drought conditions, underscoring their potential as effective soil amendments for drought mitigation. Second, the integration of hyperspectral imaging with convolutional neural network (CNN) modeling provided a robust, non-destructive framework for monitoring plant moisture status within the experimental system evaluated, enabling rapid assessment of drought responses without reliance on destructive measurements. These results demonstrate the feasibility of combining hyperspectral imaging with data-driven modeling as a high-throughput analytical framework within controlled experimental settings that complements traditional destructive moisture assessments.

Together, these findings highlight the value of combining biochar-based soil management with data-driven, non-destructive sensing approaches to study plant responses to water limitation under controlled conditions. While the HSI–CNN framework demonstrated strong capability for capturing relative differences in plant hydration within the experimental system evaluated, its broader application to field-scale crop water management will require further validation. Future work should extend this integrated approach to longer growth periods and field environments, evaluate agronomically realistic biochar application rates, and incorporate direct measurements of soil moisture dynamics and plant nutrient uptake to strengthen mechanistic understanding and practical deployment.

Acknowledgments

This work was supported and sponsored by the Natural Resources Conservation Service, US Department of Agriculture, through the grant program Partnership for Climate-Smart Commodities, grant number: NR243A750004G028.

Author contributions

Ruogu Tang: Data curation, Formal Analysis, Investigation, Methodology, Software, Validation, Visualization, Writing-original draft; Ashish Reddy Mulaka: Data curation, Investigation, Methodology, Software, Validation, Visualization; Wenxin Rong: Data curation, Investigation, Methodology, Software, Validation, Visualization, Writing-original draft; Xu Yuan: Conceptualization, Resources, Software, Supervision, Writing-review & editing; Yin Bao: Conceptualization, Resources, Software, Supervision, Writing - original draft, Writing-review & editing; Juzhong Tan: Conceptualization, Funding acquisition, Project administration, Resources, Software, Supervision, Writing-review & editing

Data availability

The data supporting the findings of this study are available within the article and its supplementary materials. Additional raw datasets are available from the corresponding author upon reasonable request.

Competing interests

The authors declare no competing interests

Reference

1. Bodner, G., Nakhforoosh, A. & Kaul, HP. Management of crop water under drought: a review. Agron. Sustain. Dev. 35 (2015) 401-442. https://doi.org/10.1007/s13593-015-0283-4

2. Mosley, L. Drought impacts on the water quality of freshwater systems; review and integration. Earth-Science Reviews. 140 (2015) 203-214. https://doi.org/10.1016/j.earscirev.2014.11.010

3. Seka, A.M., Zhang, J., Prodhan, F.A. et al. Hydrological drought impacts on water storage variations: a focus on the role of vegetation changes in the East Africa region. A systematic review. Environ Sci Pollut Res 29 (2022) 80237-80256. https://doi.org/10.1007/s11356-022-23313-0

4. Srivastav, A.L., Dhyani, R., Ranjan, M. et al. Climate-resilient strategies for sustainable management of water resources and agriculture. Environ Sci Pollut Res 28, 41576-41595 (2021).

5. Arimi., K. Climate change adaptation and resilience among vegetable farmers. International Journal of Vegetable Science, 27(5) (2022) 496-504. https://doi.org/10.1080/19315260.2020.1861160

6. Barba, J., Curiel Yuste, J., Poyatos, R. et al. Strong resilience of soil respiration components to drought-induced die-off resulting in forest secondary succession. Oecologia 182 (2016) 27-41. https://doi.org/10.1007/s00442-016-3567-8

7. Urruty, N., Tailliez-Lefebvre, D. & Huyghe, C. Stability, robustness, vulnerability and resilience of agricultural systems. A review. Agron. Sustain. Dev. 36 (2016) 15. https://doi.org/10.1007/s13593-015-0347-5

8. Salehi-Lisar, S.Y., Bakhshayeshan-Agdam, H. Agronomic Crop Responses and Tolerance to Drought Stress. In: Hasanuzzaman, M. (eds) Agronomic Crops. Springer, Singapore. 2020. https://doi.org/10.1007/978-981-15-0025-1_5

9. Teng, J., Yasufuku, N., Liu, Q. et al. Experimental evaluation and parameterization of evaporation from soil surface. Nat Hazards 73 (2014) 1405-1418. https://doi.org/10.1007/s11069-014-1138-z

10. Buchmann, C., Schaumann, G.E. Effect of water entrapment by a hydrogel on the microstructural stability of artificial soils with various clay content. Plant Soil 414 (2017) 181-198. https://doi.org/10.1007/s11104-016-3110-z

11. KhokharVoytas, A., Shahbaz, M., Maqsood, M.F. et al. Genetic modification strategies for enhancing plant resilience to abiotic stresses in the context of climate change. Funct Integr Genomics 23 (2023) 283. https://doi.org/10.1007/s10142-023-01202-0

12. Orimoloye, I.R., Belle, J.A., Olusola, A.O. et al. Spatial assessment of drought disasters, vulnerability, severity and water shortages: a potential drought disaster mitigation strategy. Nat Hazards 105 (2021) 2735-2754. https://doi.org/10.1007/s11069-020-04421-x

13. Zhang, L., Kang, C., Wu, C. et al. Optimization of Drought Limited Water Level and Operation Benefit Analysis of Large Reservoir. Water Resour Manage 36 (2022) 4677-4696. https://doi.org/10.1007/s11269-022-03271-5

14. Delval, L., Vanderborght, J. & Javaux, M. Combination of plant and soil water potential monitoring and modelling demonstrates soil-root hydraulic disconnection during drought. Plant Soil 511 (2025) 1449-1472. https://doi.org/10.1007/s11104-024-07062-2

15. Chandrashekar, H.K., Singh, G., Kaniyassery, A. et al. Nanoparticle-mediated amelioration of drought stress in plants: a systematic review. 3 Biotech 13 (2023) 336. https://doi.org/10.1007/s13205-023-03751-4

16. Das, S.K., Ghosh, G.K. & Avasthe, R. Application of biochar in agriculture and environment, and its safety issues. Biomass Conv. Bioref. 13 (2023) 1359-1369. https://doi.org/10.1007/s13399-020-01013-4

17. Roshan, A., Ghosh, D. & Maiti, S.K. How temperature affects biochar properties for application in coal mine spoils? A meta-analysis. Carbon Res. 2 (2023) 3. https://doi.org/10.1007/s44246-022-00033-1

18. Kumar, A., Bhattacharya, T., Shaikh, W.A. et al. Multifaceted applications of biochar in environmental management: a bibliometric profile. Biochar 5 (2023) 11. https://doi.org/10.1007/s42773-023-00207-z

19. Tang, R., Qiu, S., Wu, C. et al. Biochar: from agricultural waste byproducts to novel adsorbents for ammonia and micro/nanoplastics (MNPs). Biochar 7 (2025) 122. https://doi.org/10.1007/s42773-025-00554-z

20. Dotaniya, C.K., Lakaria, B.L., Sharma, Y. et al. Estimation of Potassium by Mehlich-3 Extractant Under Integrated Nutrient Management. Natl. Acad. Sci. Lett. 46 (2023) 387-390. https://doi.org/10.1007/s40009-023-01282-3

21. Buss, W., Hilber, I., Graham, C., et al. Composition of PAHs in Biochar and Implications for Biochar Production. ACS Sustainable Chem. Eng. 10 (20) (2022) 6755-6765. https://doi.org/10.1021/acssuschemeng.2c00952

22. Thomas, T., Biradar, M.S., Chimmad, V.P. et al. Growth and physiology of lettuce (*Lactuca sativa L.*) cultivars under different growing systems. Plant Physiol Rep 26 (2021) 526-534. https://doi.org/10.1007/s40502-021-00591-3

23. Sneha, Kaul, A. Hyperspectral imaging and target detection algorithms: a review. Multimed Tools Appl 81 (2022) 44141-44206. https://doi.org/10.1007/s11042-022-13235-x

24. Mohsen, S., Ali, A.M. & Emam, A. Automatic modulation recognition using CNN deep learning models. Multimed Tools Appl 83 (2024) 7035-7056. https://doi.org/10.1007/s11042-023-15814-y

25. Naidu, G., Zuva, T., Sibanda, E.M. (2023). A Review of Evaluation Metrics in Machine Learning Algorithms. In: Silhavy, R., Silhavy, P. (eds) Artificial Intelligence Application in Networks and Systems. CSOC 2023. Lecture Notes in Networks and Systems, vol 724. Springer, Cham. https://doi.org/10.1007/978-3-031-35314-7_2

26. Gezici, G., Lipani, A., Saygin, Y. et al. Evaluation metrics for measuring bias in search engine results. Inf Retrieval J 24 (2021) 85-113. https://doi.org/10.1007/s10791-020-09386-w

27. Tang, R., Tan, J. Biochar-phytagel hydrogel enhances growth, nutrient uptake, and drought resilience of lettuce microgreens. J Agric Food Res 25 (2026) 102573. https://doi.org/10.1016/j.jafr.2025.102573

28. Chaudhary, H., Dinakaran, J., Vikram, K. et al. Evaluation of physico-chemical and structural properties of biochar produced from pyrolysis of urban biowaste. J Mater Cycles Waste Manag 25 (2023) 2845-2860. https://doi.org/10.1007/s10163-023-01719-3

29. Dhar, S.A., Sakib, T.U. & Hilary, L.N. Effects of pyrolysis temperature on production and physicochemical characterization of biochar derived from coconut fiber biomass through slow pyrolysis process. Biomass Conv. Bioref. 12 (2022) 2631-2647. https://doi.org/10.1007/s13399-020-01116-y

30. Liang, X., Chen, Q., Rana, M.S. et al. Effects of soil amendments on soil fertility and fruit yield through alterations in soil carbon fractions. J Soils Sediments 21 (2021) 2628-2638. https://doi.org/10.1007/s11368-021-02932-z

31. Awais, M., Altgen, M., Mäkelä, M. et al. Quantitative prediction of moisture content distribution in acetylated wood using near-infrared hyperspectral imaging. J Mater Sci 57, 3416-3429 (2022). https://doi.org/10.1007/s10853-021-06812-2

32. Iino, H., Kawamura, S., Olivares Díaz, E. et al. Non-destructive measurement of rice amylose content using near-infrared spectroscopy for application at grain elevators and milling plants. Food Measure 18, 8275-8288 (2024). https://doi.org/10.1007/s11694-024-02800-7

33. Bao, J., Yu, M., Li, J. et al. Determination of leaf nitrogen content in apple and jujube by near-infrared spectroscopy. Sci Rep 14 (2024) 20884. https://doi.org/10.1038/s41598-024-71590-1

34. Laroche-Pinel, E., Vasquez, K.R. & Brillante, L. Assessing grapevine water status in a variably irrigated vineyard with NIR/SWIR hyperspectral imaging from UAV. Precision Agric 25 (2024) 2356-2374. https://doi.org/10.1007/s11119-024-10170-9

35. Zhang, Nn., Lu, Cy., Chen, Mj. et al. Recent advances in near-infrared II imaging technology for biological detection. J Nanobiotechnol 19 (2021) 132. https://doi.org/10.1186/s12951-021-00870-z

36. Deng, ZP., Pan, M., Niu, JT. et al. Slope reliability analysis in spatially variable soils using sliced inverse regression-based multivariate adaptive regression spline. Bull Eng Geol Environ 80 (2021) 7213-7226. https://doi.org/10.1007/s10064-021-02353-9

37. Kumar, A., Bhattacharya, T. Biochar: a sustainable solution. Environ Dev Sustain 23 (2021) 6642-6680. https://doi.org/10.1007/s10668-020-00970-0

38. Upadhyay, V., Choudhary, K.K. & Agrawal, S.B. Use of biochar as a sustainable agronomic tool, its limitations and impact on environment: a review. Discov Agric 2 (2024) 20. https://doi.org/10.1007/s44279-024-00033-2

39. Xiong, Z., Huanhuan, Z., Jing, W. et al. Physicochemical and adsorption properties of biochar from biomass-based pyrolytic polygeneration: effects of biomass species and temperature. Biochar 3 (2021) 657-670. https://doi.org/10.1007/s42773-021-00102-5

40. Seddiqi, H., Oliaei, E., Honarkar, H. et al. Cellulose and its derivatives: towards biomedical applications. Cellulose 28 (2021) 1893-1931. https://doi.org/10.1007/s10570-020-03674-w

41. Ravindiran, G., Rajamanickam, S., Janardhan, G. et al. Production and modifications of biochar to engineered materials and its application for environmental sustainability: a review. Biochar 6 (2024) 62. https://doi.org/10.1007/s42773-024-00350-1

42. Tu, P., Zhang, G., Wei, G. et al. Influence of pyrolysis temperature on the physicochemical properties of biochars obtained from herbaceous and woody plants. Bioresour. Bioprocess. 9 (2022) 131. https://doi.org/10.1186/s40643-022-00618-z

43. Zhang, N., Xing, J., Wei, L. et al. The potential of biochar to mitigate soil acidification: a global meta-analysis. Biochar 7 (2025) 49. https://doi.org/10.1007/s42773-025-00451-5

44. Su, J., Weng, X., Luo, Z. et al. Impact of Biochar on Soil Properties, Pore Water Properties, and Available Cadmium. Bull Environ Contam Toxicol 107 (2021) 544-552. https://doi.org/10.1007/s00128-021-03259-8

45. Liu, L., Fan, S. Effects of physical and chemical aging on polycyclic aromatic hydrocarbon (PAH) content and potential toxicity in rice straw biochars. Environ Sci Pollut Res 29 (2022) 57479-57489. https://doi.org/10.1007/s11356-022-19869-6

46. Singh, H., Northup, B.K., Rice, C.W. et al. Biochar applications influence soil physical and chemical properties, microbial diversity, and crop productivity: a meta-analysis. Biochar 4 (2022) 8. https://doi.org/10.1007/s42773-022-00138-1

47. Kaikiti, K., Stylianou, M. & Agapiou, A. Use of biochar for the sorption of volatile organic compounds (VOCs) emitted from cattle manure. Environ Sci Pollut Res 28, 59141-59149 (2021). https://doi.org/10.1007/s11356-020-09545-y

48. Singh, S., Luthra, N., Mandal, S. et al. Distinct Behavior of Biochar Modulating Biogeochemistry

of Salt-Affected and Acidic Soil: a Review. J Soil Sci Plant Nutr 23 (2023) 2981-2997. https://doi.org/10.1007/s42729-023-01370-9

49. Chi, W., Nan, Q., Liu, Y. et al. Stress resistance enhancing with biochar application and promotion on crop growth. Biochar 6 (2024) 43. https://doi.org/10.1007/s42773-024-00336-z

50. de Jesus Duarte, S., Cerri, C.E.P., Rittl, T.F. et al. Biochar Physical and Hydrological Characterization to Improve Soil Attributes for Plant Production. J Soil Sci Plant Nutr 23 (2023) 3051-3057. https://doi.org/10.1007/s42729-023-01273-9

51. Fakhrou, A., Kunhoth, J. & Al Maadeed, S. Smartphone-based food recognition system using multiple deep CNN models. Multimed Tools Appl 80 (2021) 33011-33032. https://doi.org/10.1007/s11042-021-11329-6

52. Kurmi, Y., Saxena, P., Kirar, B.S. et al. Deep CNN model for crops' diseases detection using leaf images. Multidim Syst Sign Process 33 (2022) 981-1000. https://doi.org/10.1007/s11045-022-00820-4

53. Thottempudi, S.G., Moulla, D.K., Agbo-Ajala, J.O., Attipoe, D., Akinyemi, L.A., Mnkandla, E. Transforming Agriculture: Disease and Pest Management Through CNN-Based Image Classification in Computer Vision. In: Woungang, I., Dhurandher, S.K. (eds) The 7th International Conference on Wireless, Intelligent and Distributed Environment for Communication. WIDECOM 2024. Lecture Notes on Data Engineering and Communications Technologies, vol 237. Springer, Cham. https://doi.org/10.1007/978-3-031-80817-3_11

Figures

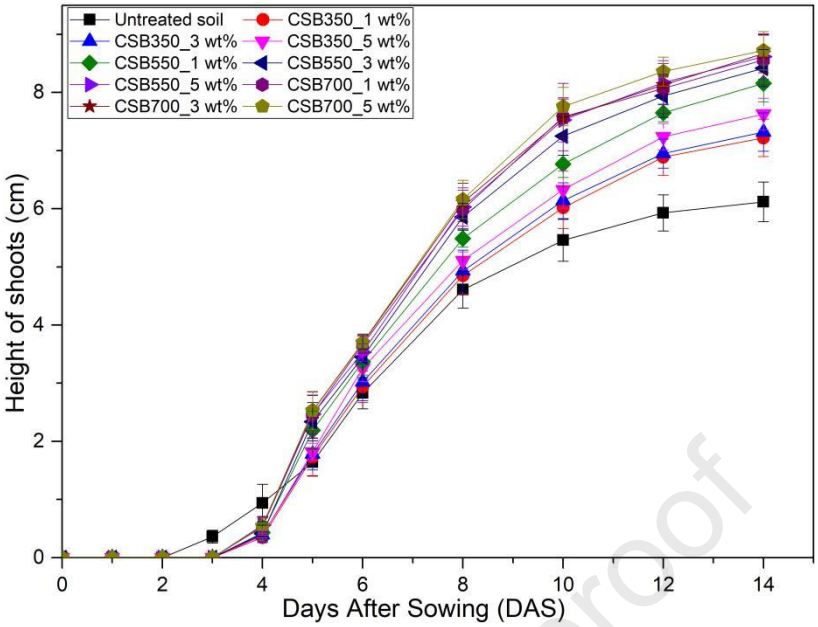

Figure 1: Shoot growth dynamics of lettuce in biochar-treated soils. Data points were presented as mean ± SD, where n=6. Tukey's HSD test was used to determine the statistical difference ($p<0.05$).

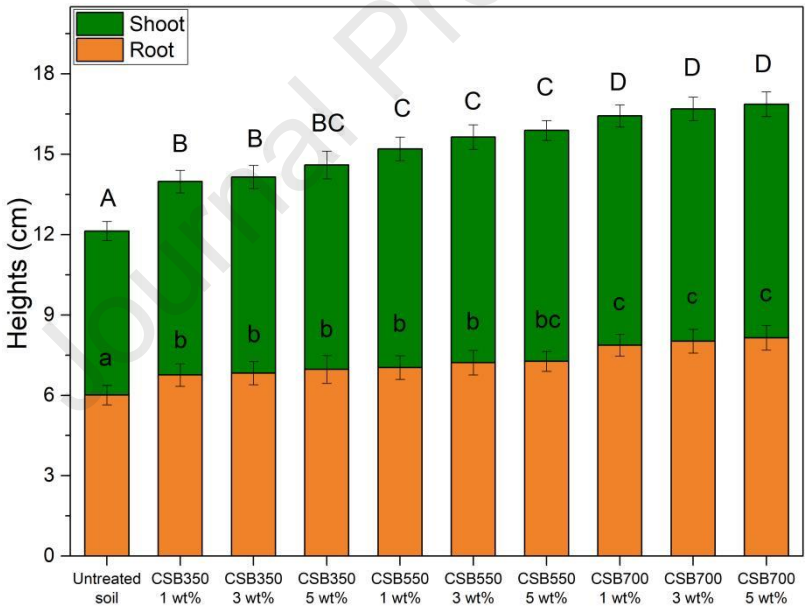

Figure 2: Shoot and root growth of lettuce seedlings on 14 days after sowing across biochar treatments. Data points were presented as mean ± SD, where n=6. Tukey's HSD test was used to determine the statistical difference ($p<0.05$). Different lower case letters indicate significant differences of root heights among all treatments, different upper case letters indicate significant differences of shoot heights among all treatments.

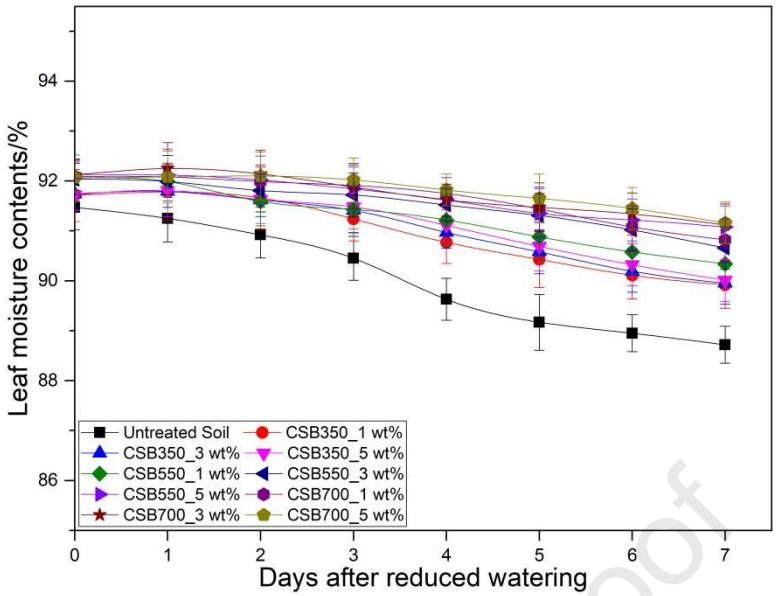

Figure 3: Leaf moisture (%) of lettuce over 7 days under water-stressed conditions.

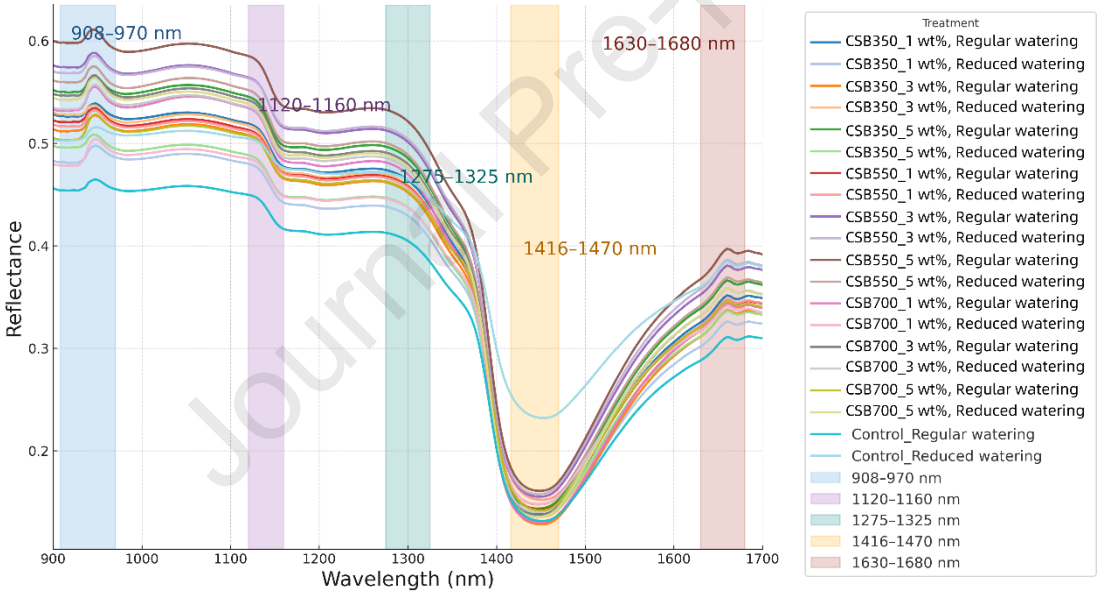

Figure 4: Average reflectance spectra of plant samples.

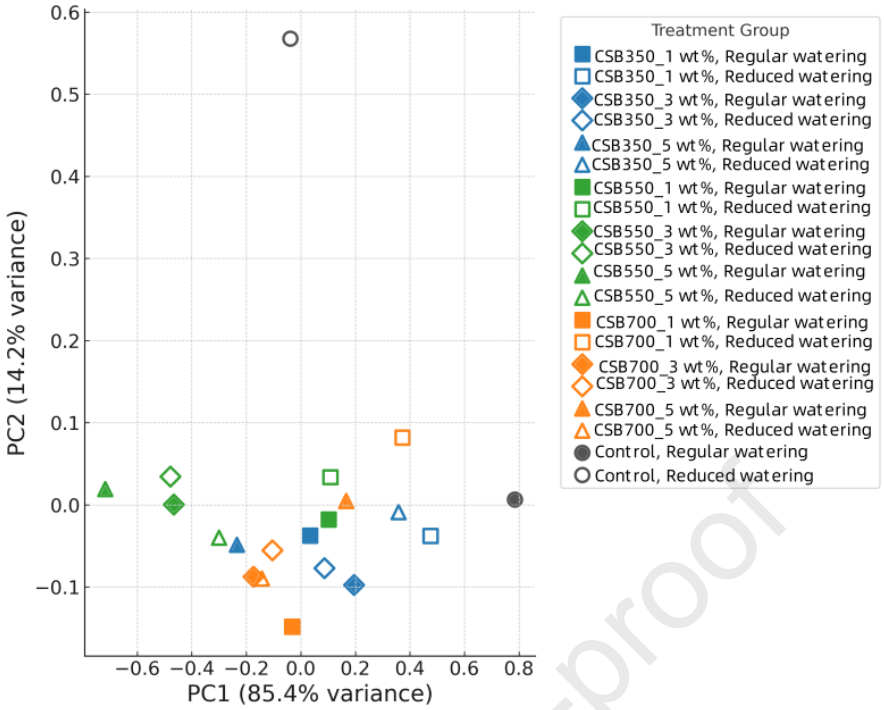

Figure 5: Principal component analysis of hyperspectral reflectance by biochar treatment.

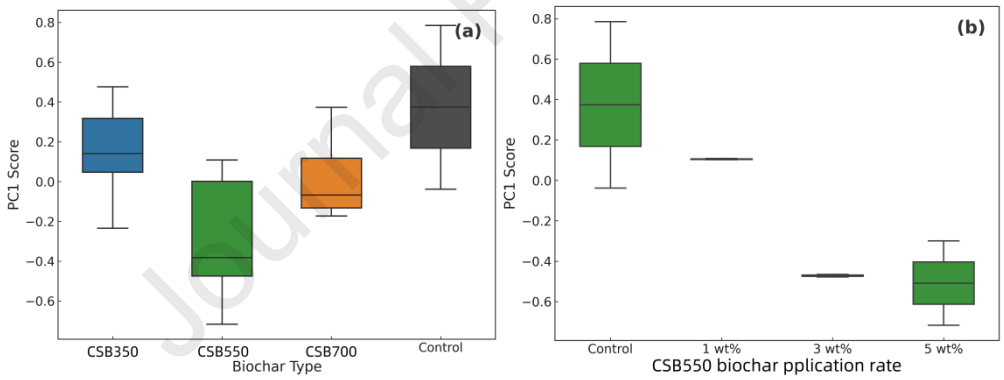

Figure 6: Distribution of PC1 scores across (a). biochar produced by different pyrolysis temperatures and (b). CSB550 application rate treatments.

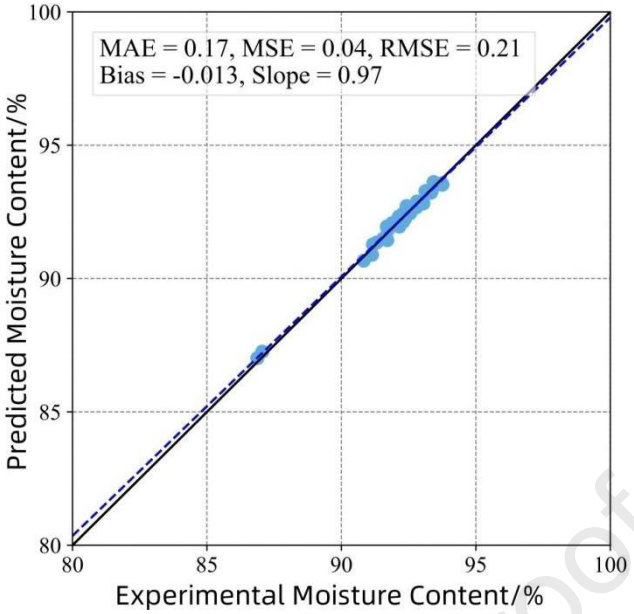

Figure 7. Scatter plot of predicted versus experimentally measured moisture content values obtained from the machine learning model. Each data point represents a single plant-level observation (n = 196), pairing hyperspectral reflectance features extracted from defined regions of interest with the corresponding gravimetrically measured moisture content. The solid black line denotes the 1:1 relationship, while the dashed blue line represents the fitted regression between predicted and measured values. Model performance metrics (MAE, MSE, RMSE, bias, and slope) are shown within the figure.

Highlights:

1. Biochar amendment improved lettuce water status under controlled drought
2. High-temperature biochar enhanced soil water retention capacity
3. HSI-CNN enabled accurate, non-destructive prediction of leaf moisture
4. Integrated framework links soil management with spectral monitoring

Declaration of Interest Statement

☒ The authors declare that they have no known competing financial interests or personal relationships that could have appeared to influence the work reported in this paper.

☐ The author is an Editorial Board Member/Editor-in-Chief/Associate Editor/Guest Editor for this journal and was not involved in the editorial review or the decision to publish this article.

☐ The authors declare the following financial interests/personal relationships which may be considered as potential competing interests: